

SCIENTIFIC REPORTS



OPEN

Magnetic induction dependence of Hall resistance in Fractional Quantum Hall Effect

Tadashi Toyoda

Quantum Hall effects (QHE) are observed in two-dimensional electron systems realised in semiconductors and graphene. In QHE the Hall resistance exhibits plateaus as a function of magnetic induction. In the fractional quantum Hall effects (FQHE) the values of the Hall resistance on plateaus are h/e^2 divided by rational fractions, where $-e$ is the electron charge and h is the Planck constant. The magnetic induction dependence of the Hall resistance is the strongest experimental evidence for FQHE. Nevertheless a quantitative theory of the magnetic induction and temperature dependence of the Hall resistance is still missing. Here we constructed a model for the Hall resistance as a function of magnetic induction, chemical potential and temperature. We assume phenomenological perturbation terms in the single-electron energy spectrum. The perturbation terms successively split a Landau level into sublevels, whose reduced degeneracies cause the fractional quantization of Hall resistance. The model yields all 75 odd-denominator fractional plateaus that have been experimentally found. The calculated magnetic induction dependence of the Hall resistance is consistent with experiments. This theory shows that the Fermi liquid theory is valid for FQHE.

The basic mechanism of the integer QHE (IQHE)^{1,2} and FQHE^{3,4} is non-uniform distribution of electron density caused by the Lorentz force acting on the electrons⁵. Theoretically the non-uniform distribution can be taken into account by using the method of subsystem^{6–10}, in which the system is divided into many strips of rectangular-shaped subsystems parallel to the direction of the bias current. The electron density in each subsystem may be different, but the chemical potential takes the same value. In each subsystem we derive the relation between the bias current and the transverse potential difference using the many-electron quantum field theory^{11–13}. The dynamics of the electrons is described in terms of the second quantised field operators that satisfy the equal-time anti-commutation relations. The Lorentz force acting on the electrons can be calculated by the Heisenberg equations for the mechanical momentum of the electrons. We assume a model Hamiltonian for the electrons in each subsystem to be $H = H_0 + H_{\text{spin}} + H_e + H_{\text{int}}$, where H_0 is the kinetic energy term with the external perpendicular magnetic field, H_{spin} is the Zeeman spin term, H_e is the coupling to the electric field, and H_{int} is the electron-electron interaction term. Calculating the statistical ensemble average of the Heisenberg equations for the mechanical momentum and assuming the steady state condition, we obtain the bias current as a function of Hall voltage in each subsystem. Assuming that the statistical ensemble average of the electron number density is given by the Fermi distribution function¹¹ and calculating the sum of the bias currents of all subsystems, we obtain the inverse of Hall resistance

$$R_H^{-1} = ecB^{-1} \sum_q D(q) \{1 + \exp[(\varepsilon_q - \mu)/k_B T]\}^{-1}, \quad (1)$$

where c , $-e$, B , μ , k_B , and T are the speed of light, electron charge, magnetic induction, chemical potential, Boltzmann constant, and temperature, respectively. The single-electron energy spectrum is denoted by ε_q with a quantum number q . The degeneracy of an energy level q is denoted by $D(q)$. It should be noted that the effects of the electron-electron interaction on ε_q can be rigorously calculated using the finite-temperature generalised Ward-Takahashi relations¹².

Department of Physics, Tokai University, 4-1-1 Kitakaname, Hiratsuka-shi, Kanagawa, 259-1292, Japan. Correspondence and requests for materials should be addressed to T.T. (email: toyoda@keyaki.cc.u-tokai.ac.jp)

Model of FQHE

To construct a model of the FQHE let us first examine the theoretical mechanism of plateaus in IQHE, which can be quantitatively explained by adopting the Landau level $\varepsilon_q = \varepsilon_{N\alpha} = \hbar\omega_c(N + 1/2 + \zeta\alpha)$ as the energy spectrum in equation (1)^{7–10}. Here $\omega_c = eB/Mc$ is the cyclotron frequency, and M is the electron effective mass. The quantum number N is a non-negative integer. The spin variable α takes the values ± 1 . The Zeeman spin term is $\hbar\omega_c\zeta\alpha$ with $\zeta = (g^*/2)(M/2M_0)$, where M_0 is the electron rest mass. The degeneracy of a Landau level with a given spin variable is $D(N, \alpha) = eB/hc \equiv D_0$. The magnetic induction B in this D_0 cancels the B -dependence of the factor ecB^{-1} in equation (1). Consequently, the inverse of Hall resistance for IQHE is

$$R_H^{-1} = e^2h^{-1} \sum_{N=0}^{\infty} \sum_{\alpha} \{1 + \exp[(\varepsilon_{N\alpha} - \mu)/k_B T]\}^{-1}. \quad (2)$$

In the zero temperature limit the inverse of Hall resistance becomes

$$\lim_{T \rightarrow 0} R_H^{-1} = e^2/h \sum_{N=0}^{\infty} \sum_{\alpha} \theta(B_{N\alpha} - B), \quad B_{N\alpha} = (\mu Mc/e\hbar)\{N + 1/2 + \alpha\zeta\}^{-1}. \quad (3)$$

This calculation shows the quantisation unit of R_H^{-1} is e^2/h because of the degeneracy of a Landau level D_0 . That is,

$$ecB^{-1}D_0 = ecB^{-1}(eB/hc) = e^2/h. \quad (4)$$

Considering the above analysis, let us inspect the Hall resistance data in the FQHE experiment reported in ref.¹⁴. The quantisation unit of R_H^{-1} on $e^2/3h$, $2e^2/3h$ and $4e^2/3h$ plateaus observed in the FQHE experiment¹⁴ is $e^2/3h$. In view of equation (4) the most plausible explanation for this is that a Landau level is split into three sublevels. Each sublevel has the degeneracy $D_1 = D_0/3$. We assume that the level-splitting is caused by a perturbation Hamiltonian \mathcal{H}'_1 , which yields new quantum numbers $m_1 = -1, 0, 1$ for sublevels. Let us call these sublevels the m_1 sublevels. The $2e^2/5h$, $2e^2/5h$, $4e^2/5h$, and $7e^2/5h$ plateaus in FQHE can be explained by assuming an additional perturbation Hamiltonian \mathcal{H}'_2 that splits each m_1 sublevel into five sublevels. Let us call these sublevels the m_2 sublevels. Each sublevel has the degeneracy $D_2 = D_1/5$. We assume that \mathcal{H}'_2 is small perturbation to \mathcal{H}'_1 . The $3e^2/7h$ and $4e^2/7h$ plateaus in FQHE can be explained by assuming an additional perturbation Hamiltonian \mathcal{H}'_3 that splits each m_2 sublevel into seven sublevels. Let us call these sublevels the m_3 sublevels. Each sublevel has the degeneracy $D_3 = D_2/7$. We assume that \mathcal{H}'_3 is small perturbation to \mathcal{H}'_2 . Hence, the quantised values of FQHE resistance at fractional plateaus can be attributed to the degeneracies of sequentially split sublevels. This analysis indicates a model energy spectrum

$$\varepsilon(N, \alpha, m) = \varepsilon_{N\alpha} + \hbar\omega_c \sum_{l=1}^{l_{\max}} \lambda_l m_l, \quad (5)$$

where m_l is an integer ranging $-l \leq m_l \leq l$. We have defined $m = (m_1, m_2, m_3, \dots)$. The parameters λ_l are assumed to satisfy the condition $|\lambda_{l+1}| < |\lambda_l|$. Using the Hall resistance formula given by equation (1), we can determine the parameters λ_l from the experiment. If λ_l are independent of B , in the zero-temperature limit, the locations of step edges on the B axis are given by equation (3) as

$$B_{N\alpha m}^{\text{FQHE}} = (\mu Mc/e\hbar) \left[N + 1/2 + \alpha\zeta + \sum_{l=1}^{l_{\max}} \lambda_l m_l \right]^{-1}. \quad (6)$$

By reading the values of $B_{N\alpha}$ from the experimental Hall resistance data at very low temperatures, it is possible to determine λ_l .

Results

Odd-denominator fractional plateaus. Because the number of possible m_l 's for a given l is $2l + 1$, the degeneracy of an energy level with quantum numbers (N, α, m) is $D(N, \alpha, m) = D_0(N, \alpha) \prod_{l=1}^{l_{\max}} (2l + 1)^{-1}$. Hence the inverse of Hall resistance for FQHE is given as

$$R_H^{-1} = e^2h^{-1} \sum_{N=0}^{\infty} \sum_{\alpha} \prod_{l=1}^{l_{\max}} (2l + 1)^{-1} \sum_m \{1 + \exp[(\varepsilon(N, \alpha, m) - \mu)/k_B T]\}^{-1}, \quad (7)$$

where we have defined $\sum_m = \sum_{m_1} \sum_{m_2} \cdots \sum_{m_{l_{\max}}}$. This formula yields the values of Hall resistance on plateaus as

$$R_H^{-1} = \frac{e^2}{h} \frac{j}{\prod_{l=1}^{l_{\max}} (2l + 1)} \quad (j = 1, 2, \dots), \quad (8)$$

where j is a positive integer. This formula yields all 75 observed odd-denominator fractional plateaus^{15,16}. It should be noted that the Hall resistance given by equation (8) is consistent with the result obtained on the basis of the fractal geometry¹⁷.

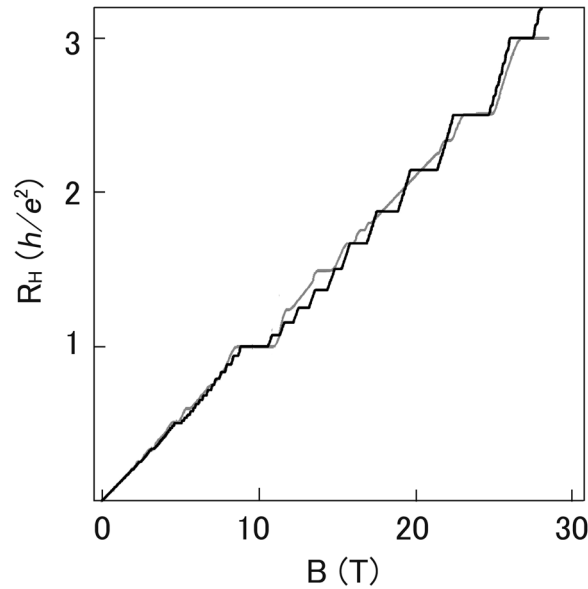


Figure 1. Theoretical Hall resistance as a function of magnetic induction. Hall resistance at $T = 85$ mK calculated by using equation (7) is plotted in black. The ordinate is Hall resistance in units of the von Klitzing constant $h/e^2 \simeq 25812.8$ ohm. The experimental Hall resistance at $T = 85$ mK from ref.¹⁴ is also plotted in gray.

Magnetic induction dependence of Hall resistance. For the practical purpose of calculating the magnetic induction dependence of Hall resistance we assume $l_{\max} = 3$ in the model energy spectrum given by equation (5) such that

$$\varepsilon(N, \alpha, m) = \varepsilon_{N\alpha} + \hbar\omega_c\{\lambda_1 m_1 + \lambda_2 m_2 + \lambda_3 m_3\}. \quad (9)$$

Note that the parameters λ_i may depend on B . For instance if we assume $\lambda_j \propto 1/\sqrt{B}$ then the energy gaps corresponding to the fractional plateaus become proportional to \sqrt{B} . Here we consider the simplest case that λ_i are independent of B . Then the three parameters λ_i in equation (9) are fitted to the experimental Hall resistance curve in ref.¹⁴. Their values are $\lambda_1 = 0.25$, $\lambda_2 = 0.14$, and $\lambda_3 = 0.003$. Considering the Hall resistance data for the IQHE experiment in ref.¹⁸, the effective g-factor is adjusted to $g^* = 12$. The effective mass is $M = 0.067 M_0$. The chemical potential is determined by the slope of experimental Hall resistance curve for weak magnetic induction. The value is $\mu = 13.14 \times 10^{-15}$ erg. The theoretical resistance curve as a function of B is plotted in Fig. 1, using equations (7) and (9) for $T = 85$ mK which is the experimental temperature in ref.¹⁴. In order to see the plateaus clearly the theoretical resistance curve for $T = 5$ mK is plotted in Fig. 2. The theoretically calculated Hall resistance plateaus $1/3, 2/5, 3/7, 4/7, 3/5, 2/3, 4/5, 1, 4/3, 7/5, 5/3,$ and 2 are consistent with the experiment¹⁴. Although the theoretical curve agrees with experiment fairly well, it seems necessary to consider the B -dependence of λ_i to improve agreement. In Fig. 3 the magnetic induction and temperature dependence of the Hall resistance is shown in a 3D plot. It shows the Hall resistance curve given by equation (7) becomes classical as temperature increases. Hence the formula (7) can yield FQHE, IQHE and classical Hall effects.

Discussion

The quantum number m_i introduced in the model perturbation energy spectrum (5) ranges $-l \leq m_i \leq l$. Therefore, it is plausible that these quantum numbers m_i and l correspond to angular momentum. Because the orbital angular momentum operators cannot be defined in the 2-dimensional space, it is necessary to consider the problem in the 3-dimensional space. We adopt (r, θ, ϕ) for the 3-dimensional polar coordinates. Then the 3-dimensional lowest Landau level (LLL) wave function is¹⁹

$$\Phi_0^{3D} = N_m \left(\frac{d^2}{a^2}\right)^{|m|/2} \exp(-z^2) \sum_{j=0}^{|m|} \frac{1}{j!} \left(1 - \frac{d^2}{2a^2}\right)^j \frac{(z^2)^{(|m|+2j)/2}}{\{2(|m|+2j)-1\}!!} \sum_{l=0}^{\infty} C(l, m; j) Y_{lm}(\theta, \phi), \quad (10)$$

where N_m is the normalisation factor, $a = \sqrt{c\hbar/eB}$ is the magnetic length, Y_{lm} is spherical harmonics, d is the thickness of the 2-dimensional system, and $z^2 = r^2/2d^2$. The expansion (10) shows that the lowest Landau level in the three-dimensional space is a superposition of angular momentum eigenstates of different l . The allowed values of m in equation (10) are only non-positive integers¹⁹. Because the quantum number m_i ranges from l to $-l$, it cannot belong to the unperturbed state given by equation (10). Therefore, the quantum number m_i possibly corresponds to new degree of freedom of the Landau orbitals in the three-dimensional space.

A model based on magnetoplasmon excitations in the three-dimensional space may explain the energy spectrum given by equation (5). The experimentally observed quantised plateaus in the magnetic induction dependence of magnetoplasmon dispersion²⁰ clearly indicate significance of magnetoplasmons in the quantum Hall

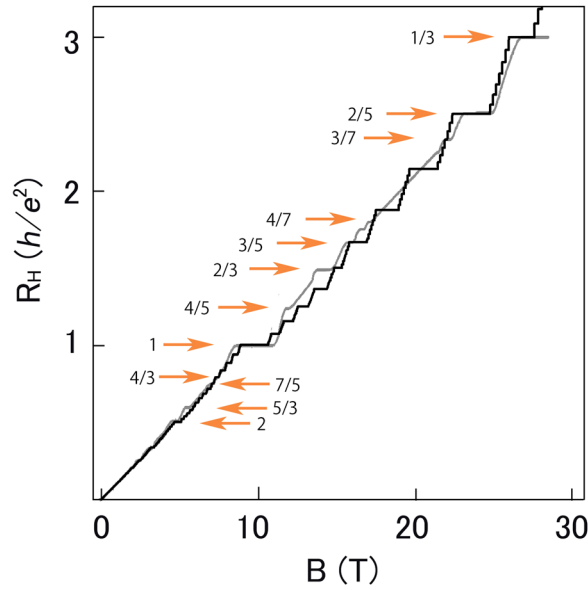


Figure 2. Theoretical Hall resistance as a function of magnetic induction. Hall resistance at $T = 5$ mK calculated by using equation (7) is plotted in black. The ordinate is Hall resistance in units of the von Klitzing constant $h/e^2 \simeq 25812.8$ ohm. The experimental Hall resistance at $T = 85$ mK from ref.¹⁴ is also plotted in grey. The horizontal arrows indicate plateaus.

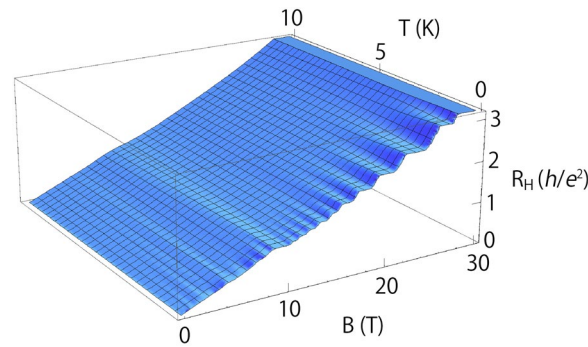


Figure 3. Theoretical Hall resistance as a function of B and T . Hall resistance calculated by using equation (7) is shown as a 3D plot for $0 < T < 10$ K and $0 < B < 30$ T. The ordinate is Hall resistance in units of the von Klitzing constant $h/e^2 \simeq 25812.8$ ohm.

effects^{6,9}. In the fractional quantum Hall regime the electron system can be regarded as a liquid of electrons in LLL orbitals. In order to examine how the magnetoplasmon fields affect the dynamics of a single-electron energy spectrum, we assume an electron P in a LLL orbital whose center is located at the origin of the coordinates. The Maxwell equations for magnetoplasmon fields have source terms due to the electrons and uniform positive background¹³. In the following discussions we shall use the Lorentz gauge and four vector notations for simplicity of mathematical expressions and to avoid the decomposition of vector fields into transverse and longitudinal components^{21,22}. Then the current densities in source terms in the Maxwell equations can be written as

$$j_\mu(x) = j_\mu^P(x) + j_\mu^{\text{induced}}(x), \tag{11}$$

where j_μ^P is due to the electron P and j_μ^{induced} is due to the other electrons. The Greek subscripts denote the components in the four-dimensional space²³. The background uniform charge is included in these terms. In the self-consistent linear response approximation (SCLRA)^{6,21,24,25} the latter is given as

$$j_\mu^{\text{induced}}(x) = \int d^4x' \sum_{\nu=0}^3 \Lambda_{\mu\nu}(x, x') A_\nu^{\text{mp}}(x'), \tag{12}$$

where $\Lambda_{\mu\nu}(x, x')$ is the retarded current-current response function^{21,26} of the electron system. The Maxwell equations for magnetoplasmon fields in the SCLRA can be written

$$(\nabla^2 - c^{-2}\partial_t^2)A_\mu^{\text{mp}}(x) + 4\pi c^{-1} \int d^4x' \sum_{\nu=0}^3 \Lambda_{\mu\nu}(x, x') A_\nu^{\text{mp}}(x') = -4\pi c^{-1} j_\mu^{\text{p}}(x). \quad (13)$$

We consider magnetoplasmons whose wavelengths are much larger than Landau radius. Then, the current density j_μ^{p} is well localised in the vicinity of the origin of the coordinates. This type of equations with a localised source term has been intensively studied in the theories of multipole fields such as radiation of electromagnetic fields^{27,28}, and it is known that spherical harmonics $Y_{lm}(\theta, \phi)$ are most relevant orthogonal basis to expand the field variables, particularly stationary waves. Therefore, the stationary modes of magnetoplasmons given by equation (13) are labeled with (l, m) . The propagator for the quantised magnetoplasmon field can be calculated from equation (13). Then the self-energy of the temperature Green function for the electron field can be expressed in terms of the magnetoplasmon propagator by virtue of the finite temperature generalised Ward-Takahashi relations^{12,29}. Consequently, the electron energy spectrum will acquire perturbation terms labeled with (l, m) .

The essential features of the SCLRA equations are determined by the retarded current-current response functions of the many-electron system^{21,26}. Therefore, in order to elaborate on this magnetoplasmon model of the spectrum given by equation (5) it is necessary to calculate these response functions, or to investigate their mathematical properties. The physical idea of this magnetoplasmon model is very similar to that of the Lamb shift in quantum electrodynamics^{30,31}. While an electron bound to an atomic orbital interacts with electromagnetic field in the Lamb shift, here an electron in LLL orbital interacts with magnetoplasmon. In both cases the reaction of the electromagnetic fields is the essential cause of the phenomena. Although magnetoplasmon is electromagnetic field, its modes are much more complicated than the electrodynamic field in the Lamb shift.

Since the discovery of the fractional quantum Hall effect, there have been a number of interesting theoretical models³². Among them the fractal geometry model¹⁷ seems to be deeply related to the present model. The Hall resistance formula given by equation (8) is consistent with the results given in ref.¹⁷. It is an interesting theoretical problem to investigate whether the current-current response functions can contain a geometrical structure such as the fractal geometry discussed in ref.¹⁷.

We explained the fractional quantised values of the Hall resistance on plateaus in terms of the degeneracies of sublevels created from Landau levels by the phenomenologically introduced perturbation in the single-electron energy spectrum. The present theory yields all 75 odd-denominator fractional values observed experimentally to date^{15,16}. The simple model with $l_{\text{max}} = 3$ yields twelve plateaus whose magnetic induction dependence is consistent with the experiment. No existing theories can yield this quantitative fit to the experiment. By calculating the temperature dependence of the Hall resistance, we plotted a 3D graph that explicitly shows how FQHE and IQHE disappear and become classical Hall effect as temperature increases. Because the Hall resistance formula (1) depends only on the single-electron energy spectrum via Fermi distributions and can explain both IQHE and FQHE, this theory clearly shows that the Fermi liquid theory^{11,12,33} is valid for IQHE and FQHE.

Methods

Derivation of Hall resistance formula. The x_1 axis is taken along the direction of the bias current, and the x_2 axis is taken along the direction of the magnetic field. Magnetic induction and electric field are given as $\mathbf{B} = (0, 0, B)$ and $\mathbf{E}^i = (E_1^i, E_2^i, 0)$, respectively. The effects of the Lorentz force on the electron currents can be calculated using the Heisenberg equations for the mechanical momentum operators

$$P_k^i = \int_{\Omega^i} \psi_\alpha^\dagger(x) \{-i\hbar\partial_k + ec^{-1}A_k\} \psi_\alpha(x), \quad (14)$$

where ψ_α and ψ_α^\dagger are the second quantized electron field operators in the Heisenberg picture. The integral notation is defined as $\int_{\Omega^i} = \int_0^L dx_1 \int_0^{\Delta L} dx_2$, where L and ΔL are the length and width of a subsystem Ω^i . We use Einstein convention for the summation over the spin variables. The superscript i denotes a subsystem. We also define the electron density operator $\rho = \psi_\alpha^\dagger \psi_\alpha$ and the electric current density operator $J_k = (-e/M) \psi_\alpha^\dagger \{-i\hbar\partial_k + (e/c)A_k\} \psi_\alpha$. The electron effective mass is denoted by M . Noting that the equal-time canonical commutators of P_k^i with H_{spin} , H_e , and H_{int} simply vanish¹⁰, i.e. $[P_k^i, H_{\text{spin}}] = [P_k^i, H_e] = [P_k^i, H_{\text{int}}] = 0$, we can readily calculate the Heisenberg equations and find

$$\partial_t P_1^i = (-eB/Mc) P_2^i - e \int_{\Omega^i} E_1^i \rho, \quad \partial_t P_2^i = (eB/Mc) P_1^i - e \int_{\Omega^i} E_2^i \rho. \quad (15)$$

Because the mechanical momentum operators and gauge current density operators satisfy the relation $P_k^i = -me^{-1} \int_{\Omega^i} J_k$, equations (15) give the equations of motion for the current density operators¹⁰. The next steps are to take the statistical mechanical ensemble average of each term in the equations and to introduce a phenomenological damping terms W_k^i , which are necessary to ensure the Ohm's law. We obtain

$$\partial_t \int_{\Omega^i} \langle J_1 \rangle^i = (-eB/Mc) \int_{\Omega^i} \langle J_2 \rangle^i + (e^2/M) \int_{\Omega^i} E_1^i \langle \rho \rangle^i + W_1^i, \quad (16)$$

and

$$\partial_t \int_{\Omega^i} \langle J_2 \rangle^i = (eB/Mc) \int_{\Omega^i} \langle J_1 \rangle^i + (e^2/M) \int_{\Omega^i} E_2^i \langle \rho \rangle^i + W_2^i. \quad (17)$$

where $\langle \dots \rangle^i$ denotes the statistical ensemble average in a subsystem Ω^i . The damping terms must vanish if there are no currents. Therefore they must satisfy the condition³³ $W_k^i = 0$ for $\int_{\Omega^i} \langle J_k \rangle^i = 0$. Considering the experimental conditions, we impose the steady state condition $\partial_t \int_{\Omega^i} \langle J_k \rangle^i = 0$ and the condition $\int_{\Omega^i} \langle J_2 \rangle^i = 0$, which gives $W_2 = 0$. Consequently equation (17) yields

$$0 = (eB/Mc) \int_{\Omega^i} \langle J_1 \rangle^i + (e^2/M) \int_{\Omega^i} E_2^i \langle \rho \rangle^i. \quad (18)$$

Although the electron-electron interaction H_{int} is rigorously included in the derivation, the electron-electron potential does not appear explicitly in this equation. The details of the damping term W_2 are not necessary. The only required condition for the damping terms is that they must vanish when there is no current.

To calculate the Hall resistance it is necessary to define macroscopic currents I_k that correspond to experimentally measurable currents. We assume $\langle \rho \rangle^i$, $\langle J_1 \rangle^i$ and $\langle J_2 \rangle^i$ in each subsystem are uniform. We first define macroscopic currents I_k^i in a subsystem Ω^i such that

$$\int_{\Omega^i} \langle J_1 \rangle^i = L_1 \Delta L \langle J_1 \rangle^i = L_1 I_1^i, \quad \int_{\Omega^i} \langle J_2 \rangle^i = L_1 \Delta L \langle J_2 \rangle^i = \Delta L I_2^i. \quad (19)$$

We also define the Hall voltage in each subsystem such that $V_2^i = -E_2^i \Delta L$. Then we have $I_1^i = (ec/B) V_2^i \rho^i$, which holds for each subsystem. By adding I_1^i from all subsystems, we obtain $I_1 = (ec/B) \sum_i V_2^i \rho^i$, where $I_1 = \sum_i I_1^i$ is the experimentally measurable macroscopic current. We assume the expectation value for the electron number density is given in terms of the Fermi distribution function $f(\varepsilon_q + \delta\varepsilon^i; T) = [1 + \exp\{(\varepsilon_q + \delta\varepsilon^i - \mu)/k_B T\}]^{-1}$. The electron energy spectrum in the subsystem Ω^i consists of an i -independent part ε_q and an i -dependent part $\delta\varepsilon_i$, where q is the quantum number of a quasi-electron state. The total current I_1 is $I_1 = ecB^{-1} \sum_i V_2^i \sum_q D(q) f(\varepsilon_q + \delta\varepsilon^i; T)$, where $D(q)$ is the degeneracy of the energy level q . The experimentally measurable Hall potential difference is $V_2 = \sum_i V_2^i$. In general the presence of $\delta\varepsilon^i$ in the Fermi distribution prohibits the evaluation of the sum over i to obtain V_2/I_1 . However, if $\delta\varepsilon^i$ is much smaller than the smallest increment of energy level ε_q , then the summation of the Fermi distributions is possible. After the summation over i we find $I_1 = ecB^{-1} V_2 \sum_q D(q) f(\varepsilon_q; T)$. This yields the inverse of Hall resistance

$$R_H^{-1} = ecB^{-1} \sum_q D(q) \{1 + \exp[(\varepsilon_q - \mu)/k_B T]\}^{-1}. \quad (20)$$

The single-electron energy spectrum is denoted by ε_q with a quantum number q . The degeneracy of energy level q is denoted by $D(q)$.

Expansion coefficients in the 3-dimensional lowest Landau level wave function. The quantum number m_l introduced in the model perturbation energy spectrum given in equation (5) ranges $-l \leq m_l \leq l$. Therefore, it is plausible that these quantum numbers m_l and l correspond to angular momentum. Because the orbital angular momentum operators cannot be defined in the 2-dimensional space, it is necessary to consider the problem in the 3-dimensional space. We adopt the vector potential $\mathbf{A} = (-Bx_2/2, Bx_1/2, 0)$. Then the lowest Landau level wave function is¹⁹

$$\Phi_0^{2D} = \frac{1}{\sqrt{2\pi}} N_{0,m}^{2D} \exp(im\phi) \exp\left(\frac{-\xi}{2}\right) \xi^{|m|/2}, \quad \xi = \frac{\rho^2}{2a^2} = \frac{r^2 \sin^2 \theta}{2a^2}. \quad (21)$$

where $N_{0,m}^{2D}$ is the normalisation factor, and $a = \sqrt{c\hbar/eB}$ is the magnetic length. Here we use (ρ, ϕ) for the 2-dimensional polar coordinates and (r, θ, ϕ) for the 3-dimensional polar coordinates. It is also necessary to consider explicitly the confining potential $V_{\text{conf.}}(x_3)$ and the 3-dimensional kinetic energy in the Hamiltonian^{26,34}. We assume the electrons are in the ground state of $V_{\text{conf.}}(x_3)$ with a simple Gaussian wave function $\chi_0 = (\sqrt{2\pi}d)^{-1} \exp[-r^2 \cos^2 \theta / 2d^2]$, where d is the thickness of the 2-dimensional system. The product of Φ_0^{2D} and χ_0 yields the 3-dimensional lowest Landau level wave function

$$\Phi_0^{3D} = N_m \left(\frac{d^2}{a^2}\right)^{|m|/2} \exp(-z^2) \sum_{j=0}^{\infty} \frac{1}{j!} \left(1 - \frac{d^2}{2a^2}\right)^j \frac{(z^2)^{(|m|+2j)/2}}{\{2(|m|+2j)-1\}!!} \sum_{l=0}^{\infty} C(l, m; j) Y_{lm}(\theta, \phi), \quad (22)$$

where N_m is the normalisation factor, Y_{lm} is spherical harmonics and $z^2 = r^2/2d^2$. The expansion coefficient $C(l, m; j)$ is calculated as

$$C(l, m; j) = \sqrt{2\pi} \left[\frac{2l+1}{2} \frac{(l-|m|)!}{(l+|m|)!} \right]^{1/2} \int_{-1}^1 dx P_l^{|m|}(x) P_{|m|+2j}^{|m|}(x) = \sqrt{2\pi} \left[\frac{2l+1}{2} \frac{(l-|m|)!}{(l+|m|)!} \right]^{1/2} I(l, |m|, j). \quad (23)$$

This integral $I(l, |m|, j)$ can be analytically evaluated³⁵. If $l+|m|$ is even and $(l-|m|)/2 \leq j$, then

$$I(l, |m|, j) = 2(-1)^{(l-|m|)/2} \frac{(2|m|+4j-1)!! (2|m|+2j)!! (l+|m|-1)!!}{(l+|m|+2j+1)!!} \left(\frac{j}{2} \right). \quad (24)$$

If $l+|m|$ is even and $j < (l-|m|)/2$, then $I(l, |m|, j) = 0$. If $l+|m|$ is odd, then $I(l, |m|, j) = 0$.

References

1. von Klitzing, K., Dorda, G. & Pepper, M. New method for high-accuracy determination of the fine-structure constant based on quantized Hall resistance. *Phys. Rev. Lett.* **45**, 494–497 (1980).
2. von Klitzing, K. The quantized Hall effect. *Rev. Mod. Phys.* **58**, 519–531 (1986).
3. Tsui, D. C., Stormer, H. L. & Gossard, A. C. Two-dimensional magnetotransport in the extreme quantum limit. *Phys. Rev. Lett.* **48**, 1559–1562 (1982).
4. Stormer, H. L., Tsui, D. C. & Gossard, A. C. The fractional quantum Hall effect. *Rev. Mod. Phys.* **71**, S299–S305 (1999).
5. Kittel, C. *Introduction to Solid State Physics, 4th edition* (John Wiley, New York, 1971).
6. Toyoda, T., Hiraiwa, N., Fukuda, T. & Koizumi, H. Plateaus in the dispersion of two-dimensional magnetoplasmons in GaAs quantum wells: theoretical evidence of an electron reservoir. *Phys. Rev. Lett.* **100**(036802), 1–4 (2008).
7. Toyoda, T. & Zhang, C. Theory of the integer quantum Hall effect in graphene. *Phys. Lett. A* **376**, 616–619 (2012).
8. Yamada, K., Uchida, T., Iizuka, J., Fujita, M. & Toyoda, T. The magnetic induction dependence of the quantum Hall resistance of graphene 2-dimensional electron system. *Solid State Commun.* **155**, 79–81 (2013).
9. Toyoda, T. *et al.* Difference between far-infrared photoconductivity spectroscopy and absorption spectroscopy: theoretical evidence of the electron reservoir mechanism. *Phys. Rev. Lett.* **111**(086801), 1–4 (2013).
10. Toyoda, T., Gudmundsson, V. & Takahashi, Y. A microscopic theory of the quantized Hall effects. *Phys. A* **132**, 164–178 (1985).
11. Abrikosov, A., Gor'kov, L. P. & Dzyaloshinskii, I. Y. *Quantum Field Theoretical Methods in Statistical Physics*. (Pergamon, London, 1965).
12. Toyoda, T. Nonperturbative canonical formulation and Ward-Takahashi relations for quantum many-body systems at finite temperatures. *Ann. Phys. (NY)* **173**, 226–245 (1987).
13. Fetter, A. L. & Walecka, J. D. *Quantum Theory of Many-Particle Systems*. (McGraw-Hill, New York, 1971).
14. Eisenstein, J. P. & Stormer, H. L. The fractional quantum Hall effect. *Science* **248**, 1510–1516 (1990).
15. Pan, W. *et al.* Fractional quantum Hall effect in the first excited Landau level: High-field low-temperature studies. *Mag Lab Reports* **15**, 9 (2015).
16. Lin, X., Du, R. & Xie, X. Recent experimental progress of fractional quantum Hall effect: 5/2 filling state and graphene. *Natl. Sci. Rev.* **1**, 564–579 (2014).
17. Mani, R. & von Klitzing, K. Fractional quantum hall effects as an example of fractal geometry in nature. *Z. Phys. B* **100**, 635–642 (1996).
18. Paalanen, M. A., Tsui, D. C. & Gossard, A. C. Quantized Hall effect at low temperatures. *Phys. Rev. B* **25**, 5566–5569 (1982).
19. Landau, L. D. & Lifshitz, E. M. *Quantum Mechanics, 2nd edition* (Pergamon, Oxford, 1965).
20. Holland, S. *et al.* Quantized dispersion of two-dimensional magnetoplasmons detected by photoconductivity spectroscopy. *Phys. Rev. Lett.* **93**(186804), 1–4 (2004).
21. Toyoda, T., Gudmundsson, V. & Takahashi, Y. Retarded transverse current-current response functions of a two-dimensional electron gas. *Phys. A* **127**, 529–548 (1984).
22. Morse, P. & Feshbach, H. *Methods of Theoretical Physics I*. (McGraw-Hill, New York, 1953).
23. Itzykson, C. & Zuber, J. *Quantum Field Theory* (McGraw-Hill, New York, 1980).
24. Toyoda, T. Self-consistent linear response approximation for quantum many-body systems. *Phys.* **253A**, 498–506 (1998).
25. Uchida, T., Hiraiwa, N., Yamada, K., Fujita, M. & Toyoda, T. Magnetic induction dependence of the dispersion of magnetoplasmon in a two-dimensional electron gas with finite layer thickness. *Int. J. Mod. Phys. B* **28**(1450044), 1–17 (2014).
26. Toyoda, T. & Fukuda, T. Transverse plasmon in a two-dimensional electron gas at finite temperature. *Phys. Rev. B* **71**(205312), 1–6 (2005).
27. Blatt, J. & Weisskopf, V. *Theoretical Nuclear Physics* (Dover Publications, New York, 2010).
28. Jackson, J. *Classical Electrodynamics* (John Wiley, New York, 1962).
29. Toyoda, T. & Ito, K. Nonperturbative approach to the self-energy of interacting electrons. *Phys. Rev. B* **64**(073104), 1–4 (2001).
30. Bethe, A. The electromagnetic shift of energy levels. *Phys. Rev.* **72**, 339–341 (1947).
31. Sakurai, J. *Advanced Quantum Mechanics* (Addison-Wesley, New York, 1967).
32. Das Sarma, S. & Pinczuk, A. *Perspectives in Quantum Hall Effects: Novel Quantum Liquids in Low-Dimensional Semiconductor Structures* (John Wiley, New York, 2007).
33. Toyoda, T. Finite-temperature Fermi-liquid theory of electrical conductivity. *Phys. Rev. A* **39**, 2659–2671 (1989).
34. Fukuda, T., Hiraiwa, N., Mitani, T. & Toyoda, T. Plasmon dispersion of a two-dimensional electron system with finite layer width. *Phys. Rev. B* **76**(033416), 1–4 (2007).
35. Akamatsu, T. (private communication).

Acknowledgements

I thank M. Yasue for thorough discussion. I thank T. Akamatsu for mathematical advice. I thank M. Fujita, K. Yamada, and T. Uchida for helpful comments.

Additional Information

Competing Interests: The author declares no competing interests.

Publisher's note: Springer Nature remains neutral with regard to jurisdictional claims in published maps and institutional affiliations.



Open Access This article is licensed under a Creative Commons Attribution 4.0 International License, which permits use, sharing, adaptation, distribution and reproduction in any medium or format, as long as you give appropriate credit to the original author(s) and the source, provide a link to the Creative Commons license, and indicate if changes were made. The images or other third party material in this article are included in the article's Creative Commons license, unless indicated otherwise in a credit line to the material. If material is not included in the article's Creative Commons license and your intended use is not permitted by statutory regulation or exceeds the permitted use, you will need to obtain permission directly from the copyright holder. To view a copy of this license, visit <http://creativecommons.org/licenses/by/4.0/>.

© The Author(s) 2018